Observation of Josephson coupling through an interlayer of antiferromagnetically ordered chromium

M. Weides,* M. Disch, H. Kohlstedt, and D. E. Bürgler
Institute of Solid State Research and JARA-Fundamentals of Future Information Technology, Research Centre Jülich, 52425 Jülich, Germany

(Received 16 June 2009; revised manuscript received 25 July 2009; published 12 August 2009)

The supercurrent transport in metallic Josephson tunnel junctions with an additional interlayer made up by chromium, being an itinerant antiferromagnet, was studied. Uniform Josephson coupling was observed as a function of the magnetic field. The supercurrent shows a weak dependence on the interlayer thickness for thin chromium layers and decays exponentially for thicker films. The diffusion constant and the coherence length in the antiferromagnet were estimated. The antiferromagnetic state of the barrier was indirectly verified using reference samples. Our results are compared to macroscopic and microscopic models.

DOI: 10.1103/PhysRevB.80.064508 PACS number(s): 74.50.+r

I. INTRODUCTION

The field of superconducting spintronics comprises interesting physical phenomena with potential applications for digital and quantum logics. The Cooper pairs leaking from a conventional superconductor (S) into a ferromagnet (F) display phase oscillation of their order parameter and a rapid decay of the amplitude over a few nanometers inside the F layer.[1] These phase oscillations are, for example, used to construct π-coupled S-F-S Josephson junctions (JJs), for which the Josephson phase in the ground state is π instead of 0, or $0-\pi$-coupled JJs, where the 0 and π coupling is locally set by a stepped F layer.[2] If the supercurrent leaks into an itinerant antiferromagnet (AF), the spin-dependent quasiparticle and Andreev reflections were shown to create low-energy bound states[3] leading for example to atomic-scale $0-\pi$ transitions of the coupling in S-AF-S type JJs.[4] S-AF multilayers are model systems for antiferromagnetic superconductors because pairing and pair breaking can be locally separated.

The $0-\pi$ phase oscillation in S-F-S JJs was verified in a number of publications[5–7] but up to now only a few experiments have been performed on S-AF-S JJs. Fast oscillations of the critical current I_c versus the magnetic field H were observed over an oxide AF interlayer and explained by canting of its magnetic moments (similar to the giant magnetoresistance effect).[8] Transport studies in metallic S-AF-S films employing a disordered FeMn alloy as AF (Ref. 9) showed deviations from the conventional $I_c(H)$ pattern, too, indicating (i) a nonuniform current distribution or (ii) a local change in the AF magnetization. Transport measurements on S-AF-S junctions based on monatomic chromium or its alloys were proposed in Refs. 4 and 10 but not realized yet.

In this paper we study the supercurrent transport through an antiferromagnetically ordered interlayer. The 3*d* metal chromium as one of the three elemental antiferromagnets (Cr, α-Mn, γ-Fe) apart from the rare earth and actinoids elements, was chosen due to its simple crystalline structure and low constrains on its atomic order for the onset of antiferromagnetic order.

The magnetic-field dependence of the critical current indicates uniform Josephson coupling over the junction area for the studied magnetic-field range up to 0.5 mT. For thin AF thicknesses the supercurrent was found to scatter strongly but to be only weakly dependent on the chromium thickness, whereas for thicker interlayer thicknesses the supercurrent decays exponentially. The supercurrent coherence length, diffusion constant, and mean-free path were determined. The magnetic properties of the Cr interlayers were verified by superconducting quantum interference device (SQUID) magnetometry using reference samples.

II. THEORY

Itinerant antiferromagnets, such as Cr with spin-density waves (SDW) propagation along special crystal directions[11] and nesting properties are described by BCS-type triplets of electron-hole pairing. Two pieces of the Fermi surface are connected by the SDW wavevector Q and the electron and hole surfaces can be superposed by translation about Q (so-called nesting condition). The orientation of SDW depends strongly on the temperature and sample properties, such as the magnetic and atomic interface structures.[11] In the low-temperature limit and for a clean interface to a FM the SDW in Cr is longitudinal, i.e., its spins and wavevector are oriented parallel and point out of plane, see Fig. 1.[12] Note that for the transport of Cooper pairs the orientation of the quantization axis is not of importance and may be orientated differently in the antiferromagnetic interlayers of our JJs. The incommensurable spin-density oscillation length of Cr at low

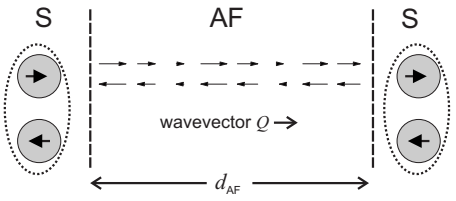

FIG. 1. Schematic representation of a S-AF-S type Josephson junction with longitudinal spin-density waves on the two antiferromagnetically coupled sublattices of the Cr interlayer (low-temperature state), for which both the propagation vector Q and the spins point out of plane.

temperature (<80 K) is about 42 monolayers or 6 nm.[11] Internal elastic strain or small grain sizes, as inevitably present in polycrystalline films, may cause the SDW to become commensurate. Bulk Cr has an AF-exchange energy E_{ex}=120 meV, a Néel temperature T_N=311 K, and an atomic magnetic moment of 0.5 μ_B at 4.2 K. The AF exchange energy E_{ex} is much larger than the superconducting gap energy and the mutually compensating magnetic moments prevent spin accumulation in the superconductor when biasing S-AF-S JJs.

The macroscopic model, based on the quasiclassical theory of an antiferromagnetic interlayer with nesting condition, such as Cr, in the dirty limit $\ell \ll \xi_{AF}$ (mean-free path ℓ and coherence length ξ_{AF}) and close to the critical temperature of the superconductor T_c, is described by the linearized Usadel equation[13] with the anomalous Green's function F_{AF} inside the AF layer[10]

$$F_{AF} = \frac{\hbar D_{AF}}{2E_{ex}} \frac{\partial^2}{\partial d_{AF}^2} F_{AF} \tag{1}$$

with an exponentially decaying solution of the form

$$F_{AF} \sim \exp(-d_{AF}/\xi_{AF}) \tag{2}$$

and coherence length $\xi_{AF}=\sqrt{\hbar D_{AF}/2E_{ex}}$ with diffusion constant $D_{AF}=v_F\ell/3$, mean-free path ℓ and AF-layer thickness d_{AF}. This ansatz is similar to the *conventional* form for ferromagnets[1] and differs by a factor of 2 from the solution used in Refs. 9 and 10. By replacing the AF layer with a F layer the magnetic exchange field E_{ex} in Eq. (1) becomes imaginary and its solution $\exp[-d_F/(\xi_F^1+i\xi_F^2)]$ contains decay and oscillations lengths $\xi_F^1=\xi_F^2=\sqrt{\hbar D_F/E_{ex}}$ (d_F: F-layer thickness). The decay length ξ_F^1 is by a factor of $\sqrt{2}$ smaller than ξ_{AF} in a AF layer.[10] The solution for F_{AF}, Eq. (2), cannot provide a change in the Josephson ground state from $0-\pi$ phase.

The microscopic model, taking the atomic magnetic order of the AF layer into account, describes the ground-state phase (0 or π) by the spin-up and spin-down reflection amplitudes. For an odd number of AF-layers π coupling can be obtained, whereas for an even number of layers the JJs are always in the 0 ground state.[4]

In Josephson junctions with an additional tunnel barrier (I), i.e., SI-AF-S JJs as studied in this paper, the low transparency interface on one side of the AF interlayer modifies the density-of-states profile in the superconductor and the Andreev reflections in the interlayer. For example, in the case of JJs with a ferromagnetic interlayer the $I_c(T,d_F)$ dependencies for S-F-S differ from SI-F-S JJs.[14] However, to our knowledge, neither (i) S-AF-S junctions with one low transparency interface, i.e., SI-AF-S JJs nor (ii) itinerant AFs with incommensurable SDWs are explicatively included in the currently available theoretical models.

III. EXPERIMENT AND DISCUSSION

The sputtered SI-AF-S multilayers consist of Nb electrodes and an AlO_x tunnel barrier (I). The AF layer was wedge shaped, thus all JJs of one set were fabricated and patterned simultaneously.[15] A 2-nm Cu buffer layer on top the *I* layer improved the growth of the antiferromagnetic Cr due to the very low solubility of Cr in Cu.[16] Thus, the stack was SIN-AF-S-type like, with the thin N layer not affecting the junction parameters as determined from SIS and SINS reference samples.[15] The AlO_x tunnel barrier was formed dynamically at 1×10^{-3} mbar (sample sets 1 and 3) or 3×10^{-1} mbar (set 2) residual oxygen pressure. Similar SI-F-S-type JJs showed a uniform increase in the *average* interlayer thickness and low-interface interdiffusion despite the polycrystalline growth.[6,15,17,18] The lithographically patterned JJs had areas of 10×5 and 50×10 μm^2, and an effective length ranging from the intermediate to the short JJ limit, i.e., $L/\lambda_J=[4\ldots0.1]$ with the Josephson penetration length $\lambda_J\sim1/\sqrt{j_c}$. Inserting a tunnel barrier in the S-AF-S stack increases the normal-state and subgap resistances. Thus, dc measurements of these samples are more feasible and the Josephson dynamics can be observed, as seen by the underdamped *I-V* characteristics in the inset of Fig. 2.

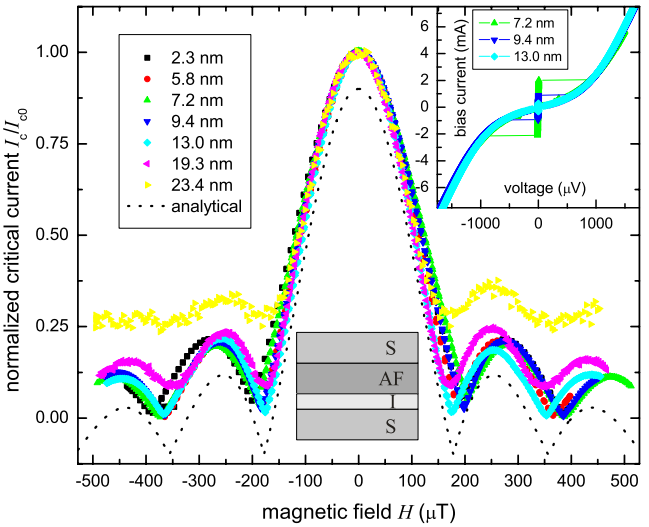

FIG. 2. (Color online) Normalized $I_c(H)$ curves and *I-V* characteristics (inset) for various d_{AF} from sets 1 and 2. The oscillation period is independent of d_{AF} and solely determined by λ_L and the junction length *L*. The magnetic fields for d_{AF}=2.3 nm and 5.8 nm were divided by the geometry factor 5 according to their shorter *L*. The side minima are lifted up due to the measurement resolution of ~1 μA. The calculated $I_c(H)$ pattern [Eq. (3), dotted line] is offset by $-0.1I_c/I_{c0}$.

The SI-AF-S JJs were zero-field cooled down to 4.2 K using μ-metal shields to suppress the external stray fields. The magnetic field *H* was applied in plane and the bias current was computer-controlled swept while measuring the voltage drop across the junction. Room-temperature voltage amplifiers were used. Both current and voltage values were automatically averaged over several hundred data points. The resolution limit is I_c=1 μA.

A. Current-voltage and magnetic-field dependence

The SI-AF-S JJs had hysteretic current-voltage characteristics up to $d_{AF}\sim15$ nm with reduced subgap features compared to normal SIS-type JJs, see inset of Fig. 2. The position

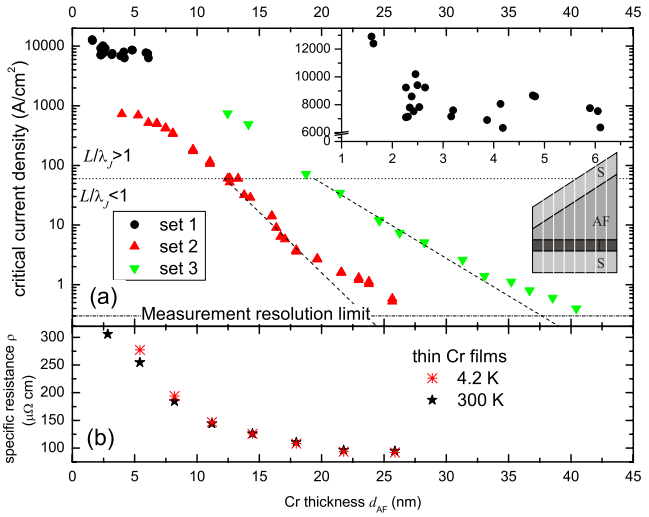

FIG. 3. (Color online) (a) $j_c(d_{\mathrm{AF}})$ of 50 $\mu\mathrm{m}^2$ (set 1) and 500 $\mu\mathrm{m}^2$ (sets 2 and 3) JJs and (b) specific resistance ρ of single Cr films. The dotted line indicates the transition from the short to the intermediate JJs length regime. The inset depicts $j_c(d_{\mathrm{AF}})$ of set 1 on a linear scale. Dashed lines are fits to Eq. (4) for short JJs from sets 2 and 3.

of zero-field and Fiske steps were as expected and were not further investigated in this work. The magnetic-field dependence of the Fraunhofern pattern for all interlayer thicknesses d_{AF} matches the short JJ model

$$I_c(H) = I_{c0}\left|\frac{\sin\left(\pi\frac{\Phi}{\Phi_0}\right)}{\pi\frac{\Phi}{\Phi_0}}\right| \tag{3}$$

with magnetic flux $\Phi=\mu_0 HL(2\lambda_L+d_I+d_{\mathrm{AF}})$ (London penetration depth λ_L). This indicates (i) the flux penetrated cross-section area $L(2\lambda_L+d_I+d_{\mathrm{AF}})\simeq 2L\lambda_L$ is unchanged for all magnetic fields, (ii) the Josephson coupling is uniform over the junction area, and (iii) the antiferromagnetic Cr layer does not modify the magnetic screening of the superconducting electrodes. Note that this is different for SI-F-S JJs, where flux focusing of the F layer, the proximity-induced increase in λ_L, and reorientation of the magnetic moments may lead to reduced oscillations periods for thicker d_F.

B. Interlayer-thickness dependence

The $j_c(d_{\mathrm{AF}})$ dependence could be measured over a range of four decades of j_c, see Fig. 3(a). The *I-V* characteristics of all junctions were symmetric and reproducible after thermal cycling, thus flux trapping effects were unlikely to occur. The function

$$j_c \sim \exp(-d_{\mathrm{AF}}/\xi_{\mathrm{AF}}) \tag{4}$$

[see Eq. (2)] was fitted to the data. To avoid current-distribution effects only small JJs were considered, yielding $\xi_{\mathrm{AF}}=2.13$ nm (set 2) and $\xi_{\mathrm{AF}}=3.44$ nm (set 3). These coherence lengths are larger than in S-AF-S JJs with highly disordered FeMn interlayer, where $\xi_{\mathrm{AF}}=1.2$ nm (after factor 2 definition correction of ξ_{AF}) was observed.[9] The measured critical-current density for JJs without chromium interlayer but the same tunnel-barrier oxidation conditions is roughly a factor of 4 larger than the extrapolated $j_c(d_{\mathrm{AF}}=0$ nm) from the sets with thinner d_{AF} (sets 1 and 2), indicating additional scattering arising at the Cr interfaces.

1. Specific resistance

To check for a change in the chromium resistivity dc transport measurements were performed on planar chromium films on SiO_2 substrates, Fig. 3(b). The specific resistance ρ of the AF layer could not be directly determined from SI-AF-S junctions as the tunnel-barrier resistance masks the serial resistance of the Cr layer. The residual resistivity ratio is nearly 1, indicating that ρ is set by the in-plane grain-boundary scattering rather than by the temperature-dependent electron-phonon interactions. However, the current transport in SI-AF-S JJs is determined by the out-of-plane resistivity, for which grain-boundary scattering is less important. The slope of $j_c(d_{\mathrm{AF}})$ changed around 20 nm (set 2), probably due to modifications in ρ. The increase in ξ_{AF} for thicker d_{AF}, i.e., set 3, is consistent with the lower $\rho(d_{\mathrm{AF}})$ for these thicknesses.

The estimation of the mean-free path ℓ in terms of the free-electron expression $\ell=\hbar/\rho e^2(\sqrt{3}\pi/n)^{2/3}$ with carrier density $n=1.6\times10^{28}$ m^{-3} yield $\ell=2.2$ nm, indicating that the dirty limit condition is not strictly fulfilled. Assuming a typical Fermi velocity for $3d$ metals $v_{\mathrm{F}}=2\times10^6$ m/s we obtain $D_{\mathrm{AF}}=14.6$ cm^2/s. Taking the bulk E_{ex} yields $\xi_{\mathrm{AF}}=2$ nm, which is fairly comparable to our ξ_{AF} determined from sets 2 and 3. This rough estimation does not account for thin-film modifications, such as interface-induced changes in the magnetic structure, interface diffusion, or domain formation, to name a few, which may vary D_{AF} or E_{ex} and hence ξ_{AF}.

C. Thin chromium interlayers

JJs with thin Cr layers ranging from 2–6 nm (set 1) have a spread of at least 30% in j_c for the same d_{AF} and a very weak or no thickness dependence, see inset of Fig. 3. The effective JJ length of these junctions is $\sim 2\lambda_J$, making long JJs effects unlikely. The spread of j_c can be related to some variations in (i) the AF-interlayer thickness, (ii) the magnetic structure, or (iii) the Josephson coupling. The normal-state resistance R_n was ~ 160 $\mathrm{m}\Omega$ for all these JJs, ruling out a variation of the junction area as a simple explanation.

1. Variation in interlayer thickness

The Cu layer at the bottom interface provides the growth of a uniform Cr layer. The strong spreads in j_c require an interlayer-thickness variation in roughly half the coherence length ξ_{AF}, i.e., ~ 1 nm, and have not been observed in previous experiments with otherwise similar SI-F-S JJs (F=$3d$ magnets) with a considerably shorter ξ_{F}.[6,17,18] The steeper slope of $j_c(d_{\mathrm{AF}})$ for thicker Cr layers makes j_c even more prone to variations in d_{AF} but such large variations in j_c were not seen for $d_{\mathrm{AF}}>6$ nm. Furthermore, the magnetic diffraction pattern indicates uniform flux penetration in the barrier

for all AF thicknesses, see Fig. 2, i.e., uniform thickness of the Cr layer.

2. Variation in the magnetic structure

The appearance of some stochastically localized magnetic states in the Cr (e.g., due to frustration) predominantly for thin AF layers would also affect the transport properties. The zero-field cool down even facilitates the formation of such magnetic defects. A JJ with a net magnetization in the interlayer deviates from the $I_c(H)$ pattern Eq. (3), as observed in SI-F-S JJs.[19] As our junctions have a standard $I_c(H)$ the local variations in the magnetic structure, if present at all, have to be small.

3. Variation in Josephson coupling

Considering the microscopic even/odd model the critical current over a JJ can be written as

$$I_c(H_x,H_y,T) = \int_{L,w} j_c^{e,o}(x,y,T)\sin\left(\phi_0 + \frac{H_x x}{L} + \frac{H_y y}{w}\right)dxdy$$

with junction length L, width w, phase ϕ_0, and $j_c^{e,o}$ being the critical-current density of even or odd layers, respectively. For an odd number of AF layers the S-AF-S JJs ground-state phase is a function of the temperature,[4] and at our measurement temperature of 4.2 K the odd-layer parts could still be in the 0-coupled ground state. Nevertheless, the j_c's for even and odd number of AF layers should differ in magnitude.

We assume that our SI-AF-S JJs have some atomic-scale roughness in d_{AF}. For similar absolute $|j_c^e|$ and $|j_c^o|$, an equal distribution of even and odd number of AF layers and the odd AF-layers mediating π coupling, the $I_c(H_x,H_y,T)$ curves would vanish at zero magnetic field due to local cancellation of the critical current. More generally, if the fraction κ of the junction area has an odd number of AF-layers mediating $\pi(0)$ coupling, the maximum critical current I_{c0} is $[(1-\kappa)|j_c^e| \mp \kappa|j_c^o|]Lw$, the integral over the axis perpendicular to the applied magnetic field (assuming a uniform distribution of even and odd layers) yields the locally averaged critical-current density $(1-\kappa)|j_c^e| \mp \kappa|j_c^o|$, and a total phase $\kappa\pi$ (if odd layers are π coupled). Thus, the $I_c(H)$ pattern still has the conventional form given by Eq. (3).

Our integral supercurrent measurement determines the averaged critical-current density and the $I_c(H)$ curves of our samples agree well with the conventional diffraction pattern, see Fig. 2. Polycrystalline samples like ours with areas being much larger than the in-plane grain size (order of 10 nm in sputtered Cu/Cr samples[20]) seem not to be suitable for the verification of the even/odd layer model by measurements of $I_c(H)$, $I_c(T)$, or $I_c(d_{\mathrm{AF}})$. The possible presence of an incommensurable SDW in Cr modifies the spin orientation and is an additional source for deviations from the even/odd model.

Nevertheless, for the thinnest layers (set 1) the parity of the Cr-layer number may set the local critical-current density due to atomic-scale roughness and thereby stochastically reduce the maximum I_{c0}, whereas for thicker layers (sets 2 and 3) the atomic-layer model looses its validity.

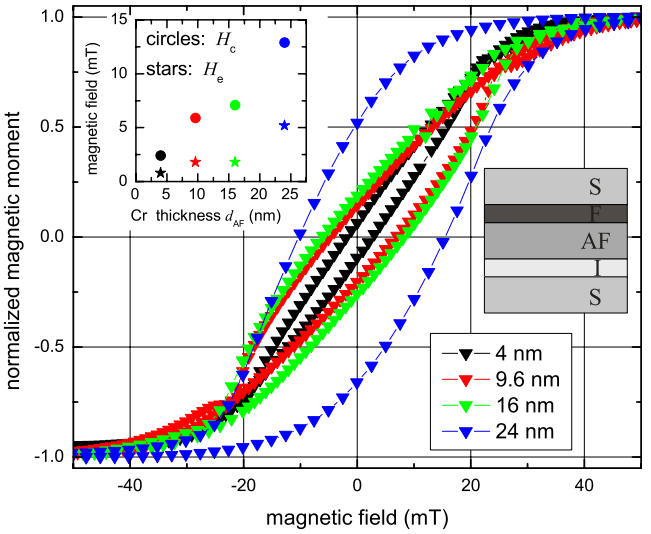

FIG. 4. (Color online) Magnetization of SI-Cr/Fe-S as a function of the in-plane magnetic field for several d_{AF} at 15 K. Exchange bias H_e (stars) and coercivity field H_c (circles) are depicted in the inset. The paramagnetic electrodes tilt the Fe magnetization toward the field axis.

D. Antiferromagnetic order of chromium

The antiferromagnetic order of the Cr layer was indirectly checked by SQUID magnetometry measurements of unstructured reference SI-Cr(4–24 nm)/Fe(3.4 nm)-S films, being otherwise similar to the SI-AF-S Josephson junctions, see Fig. 4. In AF/F bilayers the unidirectional exchange-bias effect induces for the F layer (i) a shift of the magnetic hysteresis on the field axis by the exchange-bias field H_e and (ii) an enhancement in its coercive field H_c.[11] In most cases of nonitinerant and itinerant AFs the exchange-bias field H_e is in the opposite direction than the cooling field. A positive exchange bias H_e has been observed on some samples and is caused by the microstructure and amplitude of cooling field.[21] In the case of Cr an oscillatory dependence of H_e due to reorientation of the SDW with thickness[12] and temperature[22] was reported. H_e depends strongly on the quality of samples and the properties of the interfaces, e.g., atomic-scale roughness inherent to sputtered films may weaken the exchange bias H_e. Easier experimentally detectable is H_c, which increases for thicker Cr thickness.[23]

The samples were field cooled in 1 T from room temperature down to 15 K. Figure 4 shows the widening of the hysteresis, i.e., H_c, with increasing Cr interlayer thickness and a small positive exchange bias H_e. The positive sign of the exchange bias indicates antiferromagnetic coupling at the Cr/Fe interface. The saturation magnetization does not increase for thicker Cr films and is solely contributed by the Fe film. We estimate an atomic magnetic moment of $\sim 2.2-2.3\ \mu_{\mathrm{B}}$ per atom, as expected for Fe atoms. The 4-nm Cr layer still exerts an exchange bias on the Fe layer and the coercive field is $H_c \approx 2.5$ mT, being comparable to single Fe films.[24] Polycrystalline structure, spin leaking, and paramagnetic contributions of the thick electrodes soften the magnetically hard Fe layer. The boundary conditions of Cr modify the propagation direction and the spin orientation of the

SDW, thus it may differ in SI-AF-S from the one in SI-AF/F-S samples. We note that the SI-AF/F-S samples were field cooled to verify the magnetic properties, whereas the zero-field cooled AF-JJs may show an enhanced AF-domain formation.

IV. CONCLUSIONS

In summary, transport studies of SI-AF-S junctions showed a uniform Josephson coupling, a very weak dependence of j_c on d_{AF} up to about 6 nm, and a decaying j_c for thicker d_{AF}. The antiferromagnetic order of Cr was indirectly verified using SI-AF/F-S structures. Cr has a coherence length of $\xi_{AF}=2.13-3.44$ nm.

A chromium dioxide, CrO_2, interlayer between superconducting electrodes was reported to mediate Josephson coupling over hundreds of nanometers.[25] The very weak damping of the critical current for thin Cr films ($d_{AF}<6$ nm) indicates a weak singlet pair-breaking effect for nanometer thin clusters or layers of remaining metallic chromium in the CrO_2.

In future work on SI-AF-S samples the coupling of spin-density (AF) and plasma (S) waves may be studied as the large subgap resistance facilitates dynamic transport studies. The magnetic-field and temperature dependence of I_c should be measured in epitaxial S-AF-S samples and compared to different thickness regimes in order to verify the low-temperature anomalous behavior of I_c.[3]

A thin layers of Cr may be used (i) to act as oxygen-diffusion barrier while keeping a large superconducting gap close to the Cr interface and (ii) for superconducting spin valve structures, e.g., artificial antiferromagnets of F-AF-F type[24] sandwiched by S electrodes as the damping of j_c in Cr is relatively weak.

Critical-current diffraction measurements of JJs are sensitive to magnetic remanence of the interlayer[19] and gave no indication of an intrinsic magnetic field due to the Cr layer. Both the relatively weak oxygen affinity and the exchange bias of chromium indicate that thin Cr films on top a superconducting metal may reduce the number of surface spins in SQUIDs (Ref. 26) and magnetically control the remaining spins at the interface at mK temperatures without changing the overall magnetic-field characteristics of the device.

ACKNOWLEDGMENTS

We thank A. Ustinov for stimulating discussion and D. Sprungmann for help with sample fabrication. M.W. was supported by the DFG under Project No. WE 4359/1-1 and the AvH foundation.

*Present address: Department of Physics, University of California, Santa Barbara, California 93106, USA; weides@physics.ucsb.edu

[1] A. I. Buzdin, Rev. Mod. Phys. **77**, 935 (2005).
[2] M. Weides, M. Kemmler, E. Goldobin, H. Kohlstedt, R. Waser, D. Koelle, and R. Kleiner, Phys. Rev. Lett. **97**, 247001 (2006).
[3] I. V. Bobkova, P. J. Hirschfeld, and Y. S. Barash, Phys. Rev. Lett. **94**, 037005 (2005).
[4] B. M. Andersen, I. V. Bobkova, P. J. Hirschfeld, and Y. S. Barash, Phys. Rev. Lett. **96**, 117005 (2006).
[5] V. V. Ryazanov, V. A. Oboznov, A. Y. Rusanov, A. V. Veretennikov, A. A. Golubov, and J. Aarts, Phys. Rev. Lett. **86**, 2427 (2001).
[6] M. Weides, M. Kemmler, E. Goldobin, D. Koelle, R. Kleiner, H. Kohlstedt, and A. Buzdin, Appl. Phys. Lett. **89**, 122511 (2006).
[7] T. Kontos, M. Aprili, J. Lesueur, F. Genet, B. Stephanidis, and R. Boursier, Phys. Rev. Lett. **89**, 137007 (2002).
[8] P. Komissinskiy, G. A. Ovsyannikov, I. V. Borisenko, Y. V. Kislinskii, K. Y. Constantinian, A. V. Zaitsev, and D. Winkler, Phys. Rev. Lett. **99**, 017004 (2007).
[9] C. Bell, E. J. Tarte, G. Burnell, C. W. Leung, D.-J. Kang, and M. G. Blamire, Phys. Rev. B **68**, 144517 (2003).
[10] V. N. Krivoruchko, JETP Lett. **82**, 347 (1996).
[11] H. Zabel, J. Phys.: Condens. Matter **11**, 9303 (1999).
[12] F. Y. Yang and C. L. Chien, Phys. Rev. Lett. **90**, 147201 (2003).
[13] K. L. Usadel, Phys. Rev. Lett. **25**, 507 (1970).
[14] A. S. Vasenko, A. A. Golubov, M. Y. Kupriyanov, and M. Weides, Phys. Rev. B **77**, 134507 (2008).
[15] M. Weides, K. Tillmann, and H. Kohlstedt, Physica C **437-438**, 349 (2006).
[16] T. Massalski, *Binary Alloy Phase Diagrams* (ASM International, Ohio, 1990).
[17] A. A. Bannykh, J. Pfeiffer, V. S. Stolyarov, I. E. Batov, V. V. Ryazanov, and M. Weides, Phys. Rev. B **79**, 054501 (2009).
[18] D. Sprungmann, K. Westerholt, H. Zabel, M. Weides, and H. Kohlstedt, J. Phys. D **42**, 075005 (2009).
[19] M. Weides, Appl. Phys. Lett. **93**, 052502 (2008).
[20] A. Misra, M. F. Hundley, D. Hristova, H. Kung, T. E. Mitchell, M. Nastasi, and J. D. Embury, J. Appl. Phys. **85**, 302 (1999).
[21] J. Nogués and I. K. Schuller, J. Magn. Magn. Mater. **192**, 203 (1999).
[22] J. S. Parker, L. Wang, K. A. Steiner, P. A. Crowell, and C. Leighton, Phys. Rev. Lett. **97**, 227206 (2006).
[23] F. Y. Yang and C. L. Chien, J. Appl. Phys. **93**, 6829 (2003).
[24] G. Binasch, P. Grünberg, F. Saurenbach, and W. Zinn, Phys. Rev. B **39**, 4828 (1989).
[25] R. S. Keizer, S. T. B. Goennenwein, T. M. Klapwijk, G. Miao, G. Xiao, and A. Gupta, Nature (London) **439**, 825 (2006).
[26] S. Sendelbach, D. Hover, A. Kittel, M. Muck, J. M. Martinis, and R. McDermott, Phys. Rev. Lett. **100**, 227006 (2008).